

Calibration between a Central Catadioptric Camera and a Laser Range Finder for Robotic Applications

Christopher Mei and Patrick Rives

INRIA, 2004 Route des Lucioles - BP 93, 06902 Sophia-Antipolis, Cedex - France

{christopher.mei, patrick.rives}@sophia.inria.fr

Abstract—This paper presents several methods for estimating the relative position of a central catadioptric camera (including perspective cameras) and a laser range finder in order to obtain depth information in the panoramic image. The problem is analysed from a robotic perspective and according to the available information (visible or invisible laser beam, partial calibration, drift of laser data, ...) The feasibility of the calibration is also discussed. The feature extraction process and real data are presented.

I. INTRODUCTION

The SLAM (Simultaneous Localization and Mapping) problem has been a major research topic in the robotics community since 1980's and has closely been linked with the development of sensors. Sonars and odometers are often considered as the first sensors to have led to convincing results as in the same time the theoretical fundamentals were being set [8]. Since then, laser range finders have replaced sonars when possible because of the higher precision. Techniques were also devised to make the most of these type of data (polygonal approximation, scan-matching, ...). The SLAM problem has been efficiently solved using laser in some indoor [9] and outdoor applications [7].

However some important problems need to be solved and are often directly linked to the sensors used. Localization, for example, which appears in problems like loop closing or "map choosing" are difficult with only scan data, and perspective cameras give unconvincing results. Lasers cannot help in evaluating the translation of a robot moving in a straight line in a corridor. Mapping in dynamic environments is also hard with only laser data (though not impossible [6]).

Panoramic sensors with wide fields of view [11] are becoming increasingly used. They offer the advantage of being efficient in solving problems like localization and improve motion estimation and tracking. The combination between panoramic sensors and lasers make it possible to use wide field of view vision based SLAM with the efficient depth information from the laser.

Central catadioptric sensors are a specific class of omnidirectional sensors that preserve a single effective viewpoint. This is a desirable property [11] and only certain camera and convex mirror associations make it possible [1]. Barreto [2] and Geyer [5] have proposed unified theories for the image formation of this class of sensors.

Calibration techniques for omnidirectional sensors have been at the center of a lot of research recently and some

efficient methods now exist [12]. The relationship between the 2D laser data and external properties (temperature, pressure) can be found empirically and manufacturers often provide the measurements.

This paper addresses the problem of finding the relative pose between a laser range finder and an omnidirectional sensor. The authors are not aware of any other paper analyzing this problem thoroughly, Biber and *al.* [3] give just an outline of a calibration method. The closest related work are that of Zhang and Pless [13] [14] for perspective cameras. We assume that the central catadioptric camera and the laser range finder have been previously calibrated using existing methods.

The projection model for a central catadioptric sensor is described in the first section. Different minimization problems that arise in robotics are then discussed, when the laser beam is visible (section III) and invisible (section IV) in the image plane. Section V is then dedicated to the feature extraction process and the difficulties that can arise. In the final section, the minimization problems are applied to real data and the results are analyzed.

II. UNIFIED CENTRAL CATADIOPTRIC MODEL

The class of single view point central catadioptric cameras is limited to a perspective camera combined with hyperbolic, elliptical or planar mirror or an orthographic camera with a parabolic mirror [1]. The projection in the planar mirror case is the same as the well-known perspective camera projection. Geyer [5] and Barreto [2] developed unified projection models for these cameras that separate the non linearities.

For sake of completeness we present a slightly modified version of their model. (see Fig. 1). The projection of 3D points can be done in the following steps (the parameters are in Table I) :

- 1) world points in the mirror frame are projected onto the unit sphere, $(\mathcal{X})_{\mathcal{F}_m} \longrightarrow (\mathcal{X}_s)_{\mathcal{F}_m} = \frac{\mathcal{X}}{\|\mathcal{X}\|} = s(\mathcal{X}) = (X_s, Y_s, Z_s)$
- 2) the points are then changed to a new reference frame centered in $\mathcal{C}_p = (0, 0, \xi)$, $(\mathcal{X}_s)_{\mathcal{F}_m} \longrightarrow (\mathcal{X}_s)_{\mathcal{F}_p} = (X_s, Y_s, Z_s - \xi)$
- 3) we then project the point onto the normalized plane, $\mathbf{m} = (\frac{X_s}{Z_s - \xi}, \frac{Y_s}{Z_s - \xi}, 1) = h(\mathcal{X}_s)$
- 4) the final projection involves a generalized camera projection matrix \mathbf{K} ,

$$\mathbf{p} = \mathbf{K}\mathbf{m} = \begin{bmatrix} f\eta & f\eta s & u_0 \\ 0 & f\eta r & v_0 \\ 0 & 0 & 1 \end{bmatrix} \mathbf{m} = k(\mathbf{m})$$

TABLE I
UNIFIED MODEL PARAMETERS

	ξ	η
Parabola	1	$-2p$
Hyperbola	$\frac{d}{\sqrt{d^2+4p^2}}$	$\frac{-2p}{\sqrt{d^2+4p^2}}$
Ellipse	$\frac{d}{\sqrt{d^2+4p^2}}$	$\frac{2p}{\sqrt{d^2+4p^2}}$
Planar	0	-1

d : distance between focal points
 $4p$: latus rectum

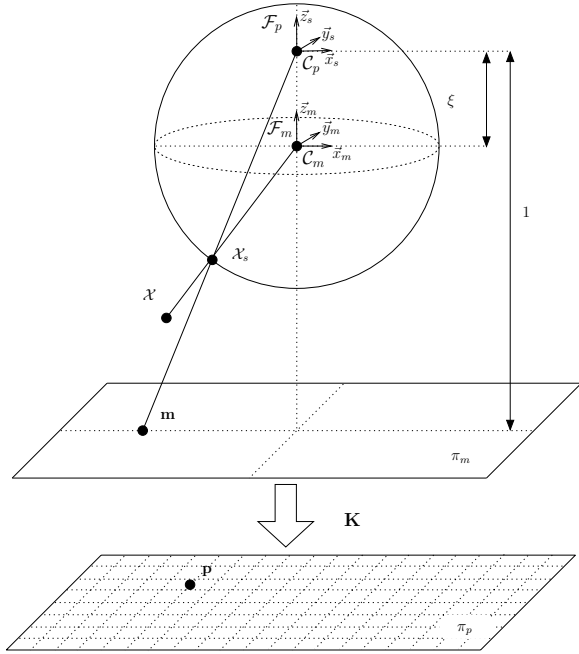


Fig. 1. Unified image formation

The function \tilde{h} is bijective and

$$\tilde{h}^{-1}(\mathbf{m}) = \begin{bmatrix} \frac{-\xi - \sqrt{1 + (1 - \xi^2)(x^2 + y^2)}}{x^2 + y^2 + 1} x \\ \frac{-\xi - \sqrt{1 + (1 - \xi^2)(x^2 + y^2)}}{x^2 + y^2 + 1} y \\ \frac{-\xi - \sqrt{1 + (1 - \xi^2)(x^2 + y^2)}}{x^2 + y^2 + 1} + \xi \end{bmatrix} \quad (1)$$

We will call lifting the calculation of the point \mathcal{X}_s corresponding to a given point \mathbf{m} (or \mathbf{p} according to the context).

III. VISIBLE LASER

Two different minimization problems will be analyzed for the case where the laser spot is visible in the image. The first considers the association between points and their images. This situation can only be obtained with laser sensors where the pan angle can be explicitly controlled. For an auto-calibration, it also imposes a static pose and cannot be done when the robot is moving.

The second part analysis the association between a laser trace (lines) and its image. This auto-calibration method can be used during the robot's displacement (even though the laser rotation will probably need to be slowed down for the beam to be visible). The disadvantage of this method comes from the difficulty of associating the data as we will see in section V.

The jacobians are specified so that a non-linear minimization method such as Levenberg-Marquardt can be used.

A. Visible laser beam

Let us assume we have n laser points $(\mathbf{l}_1, \mathbf{l}_2, \dots, \mathbf{l}_n)_{\mathcal{F}_l} \in (\mathbb{R}^2)^n$ in the laser frame and their projections $(\mathbf{p}_1, \mathbf{p}_2, \dots, \mathbf{p}_n)_{\mathcal{F}_m} \in (\mathbb{R}^2)^n$ (see Fig. 2) in the catadioptric image plane (we will discuss in Section V ways of obtaining these points).

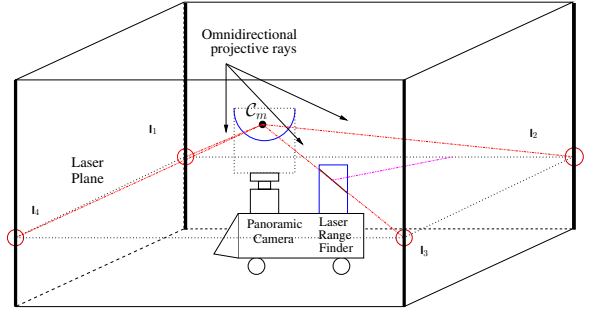


Fig. 2. Point to point association

1) *Calibration equations:* Calibrating the sensor consists in finding the rotation \mathbf{R} and translation \mathbf{T} between the laser frame (taken for example such that the laser plane corresponds to $z = 0$) and the mirror frame that minimizes the reprojection error :

$$\begin{cases} \min_{\mathbf{R}, \mathbf{T}} \frac{1}{2} \sum_{i=1}^n \|f_i(\mathbf{R}, \mathbf{T}, \mathbf{l}_i, \mathbf{p}_i)\|^2 \\ f_i(\mathbf{R}, \mathbf{T}, \mathbf{l}_i, \mathbf{p}_i) = k \circ \tilde{h}(\mathbf{R}\mathbf{l}_i + \mathbf{T}) - \mathbf{p}_i \end{cases} \quad (2)$$

It is important to note that we are here minimizing the error in the image using a euclidean metric. This metric is not theoretically a good choice because the resolution of the sensor is not uniform. A better metric is the Riemann metric associated to the sphere as it takes into account the spatial distribution. On the unit sphere, the distance between two points \mathbf{A} and \mathbf{B} is simply $\arccos(\mathbf{A}^\top \mathbf{B})$. This leads to the new minimization problem :

$$\begin{cases} \min_{\mathbf{R}, \mathbf{T}} \frac{1}{2} \sum_{i=1}^n \|g_i(\mathbf{R}, \mathbf{T}, \mathbf{l}_i, \mathbf{p}_i)\|^2 \\ g_i(\mathbf{R}, \mathbf{T}, \mathbf{l}_i, \mathbf{p}_i) = \arccos(\mathbf{A}^\top \mathbf{B}) \\ \mathbf{A} = s(\mathbf{R}\mathbf{l}_i + \mathbf{T}) \\ \mathbf{B} = \tilde{h}^{-1} \circ k^{-1}(\mathbf{p}_i) \end{cases} \quad (3)$$

2) *Jacobian:* Representing rotations by quaternions simplifies the problem of guaranteeing that the parameters represent a rotation through a simple normalization (see Annexe for more detail). $\mathbf{R}\mathbf{l}_i$ can be rewritten $\mathbf{R}\mathbf{l}_i(\mathbf{q})$ with \mathbf{q} a unit

quaternion. With n the normalization of the quaternion, we obtain the following jacobians :

$$(\nabla_{\mathbf{q}, \mathbf{T}} f)_{3 \times 7} = \nabla k \nabla h [(\nabla \mathbf{R}_{l_i} \nabla n)_{3 \times 4} \quad \mathbf{I}_{3 \times 3}] \quad (4)$$

$$(\nabla_{\mathbf{q}, \mathbf{T}} g)_{3 \times 7} = \nabla \arccos \mathbf{B}^\top \nabla s [(\nabla \mathbf{R}_{l_i} \nabla n)_{3 \times 4} \quad \mathbf{I}_{3 \times 3}] \quad (5)$$

3) *Solvability*: There are 6 unknowns and $2 \times n$ equations so at least 3 point associations are needed to solve the calibration problem.

Are 3 points sufficient ? The answer is yes if the camera center is in the laser plane but an extra point is needed otherwise. This problem is in fact the more general PnP (Perspective from n Points) problem [4]. *Four point associations are sufficient to calibrate a central catadioptric sensor (including perspective cameras) and a laser range finder.*

B. Visible laser trace

We will now analyze a slightly different problem. Instead of point associations, we have the association between a laser trace and its image (see Fig. 3).

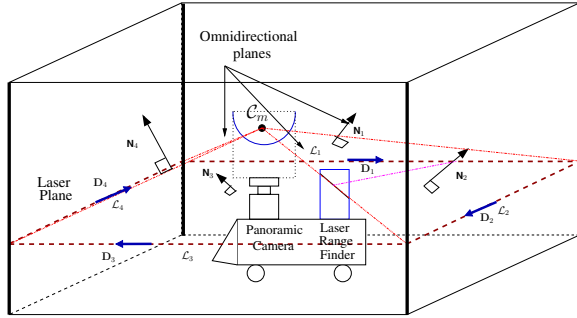


Fig. 3. Line to plane association

1) *Calibration equations*: n lines representing the image trace $(\mathcal{L}_1, \mathcal{L}_2, \dots, \mathcal{L}_n)_{\mathcal{F}_l}$ are associated to n conics in the image plane which are the images of the intersection of n planes that go through the mirror center \mathcal{C}_m . These planes have normals $(\mathbf{N}_1, \mathbf{N}_2, \dots, \mathbf{N}_n)_{\mathcal{F}_m} \in (\mathbb{R}^3)^n$ (we will discuss in Section V ways of extracting these lines and how to associate the data).

A line \mathcal{L}_i can be described by its direction vector $\mathbf{D}_i \in \mathbb{R}^3$ and a point $\mathcal{P}_i \in \mathbb{R}^3$. If we change reference frame $\{(\mathcal{L}_i)_{\mathcal{F}_l} : (\mathbf{D}_i, \mathcal{P}_i)\} \rightarrow \{(\mathcal{L}_i)_{\mathcal{F}_m} : (\mathbf{R}\mathbf{D}_i, \mathbf{R}\mathcal{P}_i + \mathbf{T})\}$.

This leads to the constraints :

$$\begin{cases} \mathbf{N}_i^\top \mathbf{R}\mathbf{D}_i = 0 \\ \mathbf{N}_i^\top (\mathbf{R}\mathcal{P}_i + \mathbf{T}) = 0 \end{cases}$$

Thus we have the following decoupled minimization problem :

$$\begin{cases} \min_{\mathbf{R}} \frac{1}{2} \sum_{i=1}^n \|t_i(\mathbf{R}, \mathbf{N}_i, \mathbf{D}_i)\|^2 \\ t_i(\mathbf{R}, \mathbf{N}_i, \mathbf{D}_i) = \mathbf{N}_i^\top \mathbf{R}\mathbf{D}_i \\ \mathbf{N}\mathbf{T} = -\mathbf{P} \end{cases} \quad (6)$$

with $\mathbf{N} = [\mathbf{N}_1 \dots \mathbf{N}_n]^\top$ and $\mathbf{P} = [\mathbf{R}\mathcal{P}_1 \dots \mathbf{R}\mathcal{P}_n]^\top$

The second linear problem can easily be solved by using the pseudo-inverse : $\mathbf{T} = -(\mathbf{N}^\top \mathbf{N})^{-1} \mathbf{N}^\top \mathbf{P}$.

2) *Jacobian for the rotation extraction*: Yet again we can parametrize $\mathbf{R}\mathbf{D}_i$ by a quaternion, we note the matrix $\mathbf{R}_{\mathbf{D}_i}(\mathbf{q})$.

$$(\nabla_{\mathbf{q}} t_i)_{1 \times 4} = \mathbf{N}_i^\top \nabla \mathbf{R}_{\mathbf{D}_i} \nabla n$$

IV. INVISIBLE LASER

The more complex problem of calibrating the sensor when the laser beam is not observable in the image will now be discussed.

A. Calibration from planes

The work from Zhang and Pless [14] can be adapted to central catadioptric sensors. It is assumed that a calibration grid is seen in the image and appears in the laser range scan (see Fig. 4).

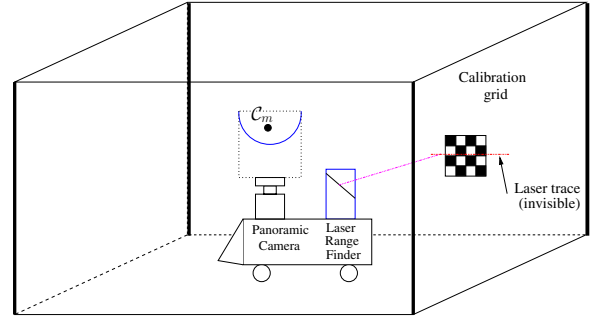


Fig. 4. Association between a calibration grid and a laser trace

The minimization problem described in section III-A can be used to solve the pose estimation problem of a grid seen in the image plane. Thus the equation of the plane $\pi_i : \mathbf{N}_i, d_i$ can be obtained (d_i represents the distance from the camera to the calibration plane).

The constraints are the same as in section III-B except that the distance from the planes to the camera is no longer 0 :

$$\begin{cases} \mathbf{N}_i^\top \mathbf{R}\mathbf{D}_i = 0 \\ \mathbf{N}_i^\top (\mathbf{R}\mathcal{P}_i + \mathbf{T}) = \mathbf{d}_i \end{cases}$$

The same approach as before can be used for the minimization with $\mathbf{P} = [\mathbf{R}\mathcal{P}_1 - d_1 \quad \mathbf{R}\mathcal{P}_2 - d_2 \quad \dots \quad \mathbf{R}\mathcal{P}_n - d_n]^\top$.

If instead of using lines, the laser points are used directly with $\mathbf{l}_{ij} \in \mathcal{L}_i$, we obtain :

$$\begin{cases} \min_{\mathbf{R}, \mathbf{T}} \frac{1}{2} \sum_{i,j} \|w_{ij}(\mathbf{N}_i, \mathbf{d}_i, \mathbf{R}, \mathbf{T})\|^2 \\ w_{ij} = \mathbf{N}_i^\top (\mathbf{R}\mathbf{l}_{ij} + \mathbf{T}) - \mathbf{d}_i \end{cases} \quad (7)$$

with the following jacobian :

$$(\nabla_{\mathbf{q}, \mathbf{T}} w_{ij})_{1 \times 7} = \mathbf{N}_i^\top [(\nabla \mathbf{R}_{\mathbf{l}_{ij}} \nabla n)_{3 \times 4} \quad \mathbf{I}_{3 \times 3}]$$

B. General case

Under the hypothesis that edges in the image correspond to edges in the laser scan (see Fig. 5) is it possible to generate enough constraints to calibrate the sensor entirely (ie. estimate \mathbf{R} and \mathbf{T}) ?

The minimization problem can be rewritten as the association between the 3D points $(\mathcal{X}_1, \mathcal{X}_2, \dots, \mathcal{X}_n)$ and the laser

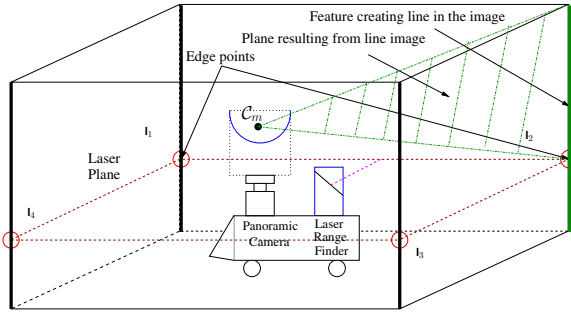


Fig. 5. Association between edge features

points (without loss of generality, we can assume that the plane is in $Z = 0$). The points \mathcal{X}_i belong to the planes parametrized by $\mathbf{N}_i : \mathbf{N}_i^\top \mathcal{X}_i = 0$

$$\begin{cases} \begin{bmatrix} \mathbf{R} & \mathbf{T} \\ 0 & 1 \end{bmatrix} \begin{bmatrix} \mathcal{X}_1 & \dots & \mathcal{X}_n \\ 1 & \dots & 1 \end{bmatrix} = \begin{bmatrix} \mathbf{l}_1 & \dots & \mathbf{l}_n \\ 0 & \dots & 0 \\ 1 & \dots & 1 \end{bmatrix} \\ \mathbf{N}_i^\top \mathcal{X}_i = 0 \end{cases} \quad (8)$$

In this case, there are $6 + 3 \times n$ unknowns and $3 \times n + n$ equations so at least 6 points and corresponding planes are needed to solve the calibration problem. The condition $\text{rank}(\mathbf{N}) = 3$ must also be satisfied or a translation direction is unsatisfied. In Fig. 5, the four vertical lines are parallel, $\text{rank}(\mathbf{N}) = 2$ and the translation along these lines is not constrained.

Are these two conditions sufficient? The answer is no and worse than that, however many points and plane associations, three parameters are always missing. The proof can be found in the Appendix. The reason comes from the coplanarity of the l_i points.

Auto-calibration between a central catadioptric sensor and a laser range finder is impossible in the general case (without 3D point associations).

To obtain convergence towards the solution, it is necessary to know the association between three planes containing three different 3D points that are not in the laser plane and their position with respect to the laser plane. To obtain these points, the robot must move from a known value in a direction different to the laser plane using for example the equations derived in [13] which can easily be adapted to the omnidirectional case. This also means that to obtain the translation value on the vertical axis, if the laser plane is horizontal, the robot must move vertically (drone) which is of course impossible for standard mobile robots.

V. DATA EXTRACTION AND ASSOCIATION

A. Visible laser beam

A method to extract the data in the case of a visible laser beam is to take a reference image I_{ref} with the laser turned off. After having given an angular position to the laser a new image I_c can be taken. The laser point is then simply the

maximum intensity value in the difference image $I_c - I_{ref}$. To improve the robustness, the maximum can be looked for in a window based on an estimate of the laser point reprojection. The *skeletonize* morphological operation can also be used to reduce the signal to a dot in the difference image.

B. Visible laser trace

To obtain a strong signal corresponding to the laser, the rotation speed needs to be turned down. Several images are then taken and the difference between a reference image and a image with the laser turned on is accumulated. To avoid obtaining a trace several pixels wide, we use a line thinning algorithm (eg. the *skeletonize* morphological operation).

The conics corresponding to the image of the laser trace can then be extracted using the randomized hough transform [10] (see Fig. 11). Similarly we can extract the lines from the laser scan (see Fig. 10).

The problem then consists in associating the lines. If there are n_1 omni-lines and n_2 laser-lines and it is assumed that there are p line associations, $p C_{n_1}^p C_{n_2}^p$ values need to be checked. This is a computationally expensive task, it is also made harder by the difficulty of estimating the correctness of an association. A possible approach is to find the best association for 4 lines and then to gradually increase the size of the associated sets.

VI. RESULTS

The calibration of the camera was done using a toolbox available on Internet¹ and the images were corrected for lens distortion.

A. Visible laser beam

To validate the extraction process, 10 auto-calibrations were done. The translation estimation for each calibration is presented in Fig. 6 and the rotation in Fig. 7, the lines correspond to the global calibration results. Table I summarizes the estimation of the parameters.

The method gave a robust estimation of the translation and the rotation except in the first case (which was removed for the global parameter estimation). In a real-world auto-calibration phase, these type of errors could easily be detected. For data fusion, the most important information is the error in pixels which was just over a pixel. The standard deviation was quite high due to outliers.

Fig. 8 shows one of the laser scans. The extracted laser spots are shown in Fig. 11. The points reprojected after the rotation and translation estimate are indicated in '+' marks.

B. Visible laser trace

The calibration using only the laser trace did not give such good results. Table III summarizes the results over two images containing 6 lines each. The results are unconvincing, probably due to the accumulation error from the line estimates and to the "loosely" constrained minimization problem. This approach

¹<http://www-sop.inria.fr/icare/personnel/Christopher.Mei/Toolbox.html>

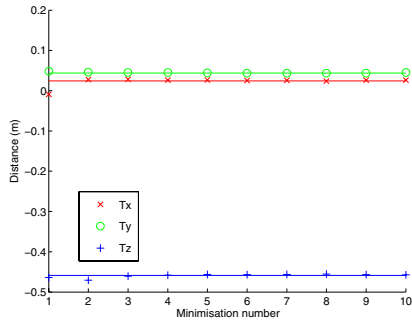


Fig. 6. Estimation of the translation

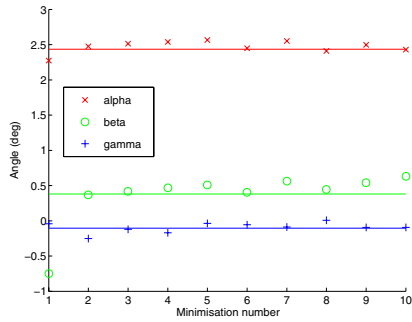


Fig. 7. Estimation of the rotation

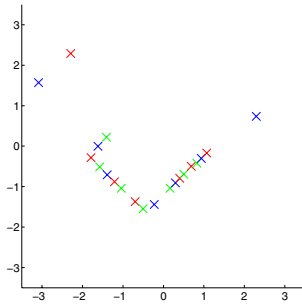


Fig. 8. Laser points

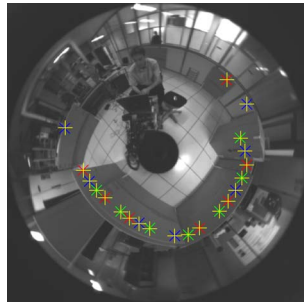


Fig. 9. Reprojection of the laser scan

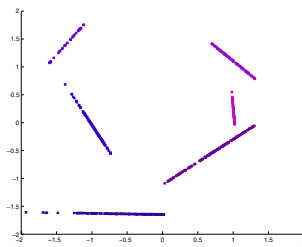


Fig. 10. Laser lines

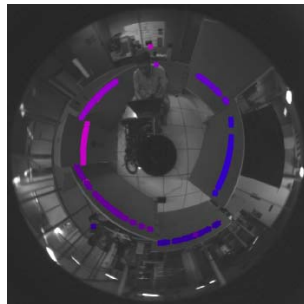


Fig. 11. Extraction of the laser trace

TABLE II
PARAMETER ESTIMATION

T	σ	R (deg)	σ	Pixel error	σ
0.0257	0.0011	2.4902	0.0507		
0.0440	0.00062	0.4944	0.0827	1.367	1.354
-0.4574	0.0016	-0.0888	0.0496		

proved also to be difficult to put into place in an autonomous way, as the calibration can only be done in an environment with enough planes to constrain the system.

TABLE III
PARAMETER ESTIMATION

T	Minimization error	R (deg)	Minimization error
-0.032	0.0037	4.259	0.0012
0.051		-0.300	
-0.439		0.864	

C. Calibration from planes

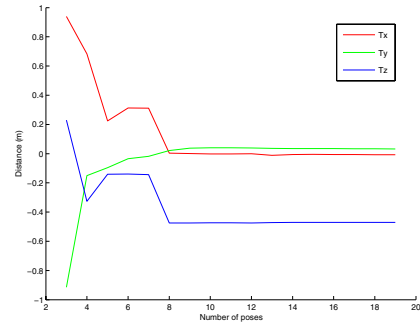


Fig. 12. Estimation of the translation

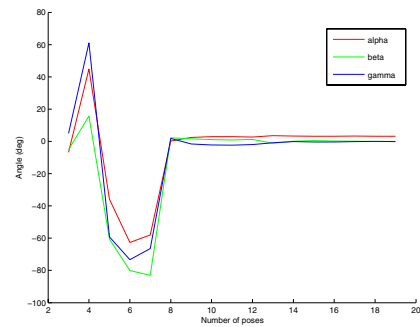


Fig. 13. Estimation of the rotation

The calibration from planes was also evaluated. Equation 7 was used for the minimisation. To extract the signal corresponding to the planes in the image scan, only the points that contributed to lines when using a randomized hough transform were kept.

The evaluation was done on 19 associations between the visible planes and their trace in the laser scan. The estimation of the rotation and translation improved regularly with the amount of poses as shown in Fig. 12 and Fig. 13. We obtained $\mathbf{T} = [-0.0074, 0.0321, -0.471]$ and $\mathbf{R} = [3.147, 0.048, -0.099]$ which is compatible with the previous calibrations. Figure 14 shows some of the planes and their associated laser points in the camera frame after calibration.

This method has the advantage of giving good results without needing to see the laser beam in the image.

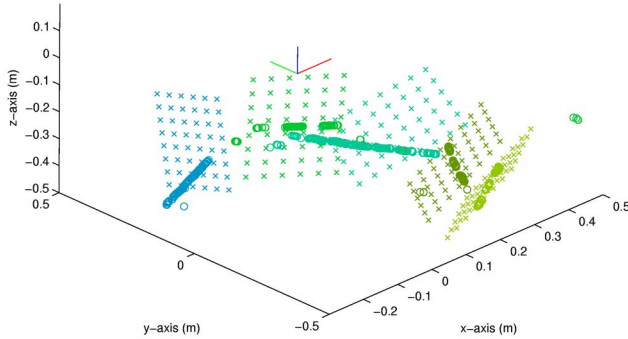


Fig. 14. Planes and associated laser points (camera frame)

APPENDIX

Rotation parametrization with quaternions

Let $\mathbf{X} = [x \ y \ z]^T$ and $\mathbf{q} = [q_0 \ q_1 \ q_2 \ q_3]^T$:

$$\mathbf{R}\mathbf{X} = \mathbf{R}_{\mathbf{X}}(\mathbf{q}) = \begin{bmatrix} \mathbf{R}_{\mathbf{X}}^1(\mathbf{q}) & \mathbf{R}_{\mathbf{X}}^2(\mathbf{q}) & \mathbf{R}_{\mathbf{X}}^3(\mathbf{q}) \end{bmatrix}^T$$

with :

$$\mathbf{R}_{\mathbf{X}}^1(\mathbf{q}) = (q_0^2 + q_1^2 - q_2^2 - q_3^2)x + 2(-q_0q_3 + q_1q_2)y + \dots + 2(q_0q_2 + q_1q_3)z$$

$$\mathbf{R}_{\mathbf{X}}^2(\mathbf{q}) = 2(q_0q_3 + q_1q_2)x + (q_0^2 - q_1^2 + q_2^2 - q_3^2)y + \dots + 2(-q_0q_1 + q_2q_3)z$$

$$\mathbf{R}_{\mathbf{X}}^3(\mathbf{q}) = 2(-q_0q_2 + q_1q_3)x + 2(q_0q_1 + q_2q_3)y + \dots + (q_0^2 - q_1^2 - q_2^2 + q_3^2)z$$

General calibration

Equation (8) aims at finding the isometry (\mathbf{R}, \mathbf{D}) that transforms a n-tuple $(\mathcal{X}_1, \dots, \mathcal{X}_n)$ into the polygon defined by $(\mathbf{l}_1, \dots, \mathbf{l}_n)$. Are the constraints defined on the \mathcal{X} s through the planes with normals \mathbf{N} s sufficient to define uniquely the $(\mathcal{X}_1, \dots, \mathcal{X}_n)$ polygon ? The proof established here uses an iterative geometric construction. In brackets are indicated the difference between the number of equations and the number of unknowns.

With 1 point, we have 1 equation but 3 unknowns (-2).

With 2 points, if $\text{rank}(\mathbf{N}_1, \mathbf{N}_2) = 2$, we have 2 equations from the normals and 1 equation from the distance but 6 unknowns (-3).

With 3 points, if $\text{rank}(\mathbf{N}_1, \mathbf{N}_2, \mathbf{N}_3) = 3$, we have 3 equations from the normals and 3 distances - these equations

are all independent - and 9 unknowns (-3) (see Fig. 15 drawn in the plane defined by the three points).

With an extra point \mathcal{X}_4 , if we add three distance constraints (see Fig. 16) two possibilities occur : either they are sufficient to define \mathcal{X}_4 uniquely which is the case if the solution is planar, or there are two possible points which are at the intersection of the three spheres centered at $\mathcal{X}_1, \mathcal{X}_2$ and \mathcal{X}_3 . A plane defined by \mathcal{X}_4 which does not contain the two points will define uniquely \mathcal{X}_4 (-2).

If the solution is not planar, this reasoning can be applied recursively and for $n = 6$ with specific \mathbf{N} s, the system will have a unique solution.

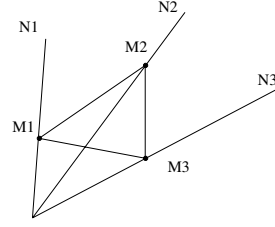


Fig. 15. Constraints on three points in a plane

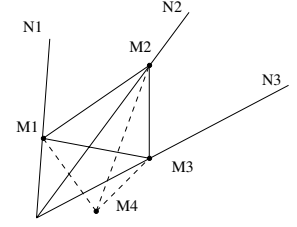


Fig. 16. Distance constraints on a fourth point

In the case of the laser data, the solution $(\mathbf{l}_1, \dots, \mathbf{l}_n)$ is planar so 3 extra constraints are missing to solve the system.

REFERENCES

- [1] Simon Baker and Shree K. Nayar. A theory of catadioptric image formation. In *ICCV*, pages 35–42, 1998.
- [2] Joao P. Barreto and Helder Araujo. Issues on the geometry of central catadioptric image formation. In *CVPR*, 2001.
- [3] Peter Biber, Henrik Andreasson, Tom Duckett, and Andreas Schilling. 3d modeling of indoor environments by a mobile robot with a laser scanner and panoramic camera. In *IROS*, 2004.
- [4] Martin A. Fischler and Robert C. Bolles. Random sample consensus: a paradigm for model fitting with applications to image analysis and automated cartography. *Commun. ACM*, 24(6):381–395, 1981.
- [5] C. Geyer and K. Daniilidis. A unifying theory for central panoramic systems and practical implications. In *ECCV*, 2000.
- [6] D. Hahnel, D. Schulz, and W. Burgard. Map building with mobile robots in populated environments. In *IROS*, 2002.
- [7] Y. Liu and S. Thrun. Results for outdoor-SLAM using sparse extended information filters. In *ICRA*, 2003.
- [8] R. C. Smith and P. Cheeseman. On the representation and estimation of spatial uncertainty. *International Journal of Robotics Research*, 1986.
- [9] A.C. Victorino, P. Rives, and P. Borrelly. Safe navigation using sensor-based control techniques for indoor mobile robots. *International Journal of Robotics Research*, 2002.
- [10] L. Xu and E. Oja. Randomized hough transform (rht) : Basic mechanisms, algorithms, and computational complexities. *CVGIP*, 57(2):131–154, 1993.
- [11] Yasushi Yagi. Omnidirectional sensing and its applications. *IEICE Trans, on Information and Systems*, E82-D(3):568–579, 1999.
- [12] Xianghua Ying and Zhanyi Hu. Catadioptric camera calibration using geometric invariants. *IEEE Transactions on Pattern Analysis and Machine Intelligence*, 26(10):1260–1271, 2004.
- [13] Qilong Zhang and Robert Pless. Constraints for heterogenous sensor auto-calibration. In *IEEE CVPR Workshop on Real-Time 3D Sensors and their Use*, 2004.
- [14] Qilong Zhang and Robert Pless. Extrinsic calibration for a camera and laser ranger finder (improves camera intrinsic calibration). In *IEEE/RSJ International Conference on Intelligent Robots and Systems*, 2004.